Indoor measurements by dual tripole antennas

Jesús Gutiérrez[1], Aamir Habib[2,3]and Markus Rupp[2]

[1]Dept. of Communications Engineering, University of Cantabria, Santander, Spain 39005
Email: {jesusgt}@gtas.dicom.unican.es

[2]Vienna University of Technology
Institute of Telecommunications
Gußhausstraße 25/389, A-1040 Vienna
Email: {ahabib,markus.rupp}@nt.tuwien.ac.at

[3]Institute of Space Technology
Electrical Engineering Department
1, Islamabad Highway, 44000 Islamabad
Email: {aamir.habib}@ist.edu.pk

***Abstract*—We present in this paper indoor measurements at $2.45\,\mathrm{GHz}$ of a tripole antenna pair and investigate typical channel characteristics that include the antenna elements. Each of the two antenna arrays consists of three orthogonal co-located dipoles promising high capacity, irrelevant of their orientation. The impact of classic parameters related to polarization, correlation and time dispersion are analyzed in order to get an idea of the performance that this real multiple-input multiple-output (MIMO) system could offer.**

I. Introduction

The existence of mutual coupling effects impacts on the scattering and radiating characteristics of antenna arrays, affecting the performance of multiple-input multiple-output (MIMO) communication systems [1], [2]. In most cases coupling is detrimental to the antenna operation, although there are some examples in which its presence can be beneficial.

In orthogonal co-located MIMO systems, one of the most significant factors in establishing the level of mutual coupling, characterized by the so called cross polar discrimination (XPD), is whether or not all aspects of the antenna structure are truly orthogonal. Transmission systems with such antennas allow achieving higher capacity by utilizing spatial and polarization diversity [3], [4]. Also, their actual performance is strongly dependent on the characteristics of the propagation channel [5]. Therefore, low mutual coupling is an important feature to reduce the existing correlation among antenna elements along with the spatial correlation properties of the channel. In this paper, we aim at analyzing the characteristics of the 3×3 MIMO channel using a tripole pair based on an indoor measurement campaign at $2.45\,\mathrm{GHz}$. Different parameters related to polarization, spatial and temporal domains have been extracted and discussed to fully characterize the environment.

The remaining sections of this paper are organized as follows: An introduction and background on orthogonal MIMO channels is described in Section II. The equipment and measurement setup are presented in Section III. Section IV describes the analyzed parameters along with the obtained results from the measurement campaign. Finally, the conclusions are put forward in Section V.

II. Crossed dipole model

The use of co-located orthogonal dipoles in a transmission RF system ensures significantly different properties of the co-polar subchannels, dipoles with the same orientation at both sides, when compared to those of the cross-polar subchannels (different orientation). Fig. 1 represents a cross dipole scheme assuming three co-located antenna elements at both link ends.

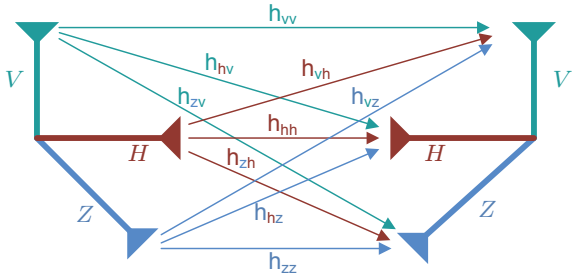

Fig. 1. Configuration of triple-polarized system.

The entire MIMO channel can be described by a 3×3 matrix $\mathbf{H}$, whose elements h_{ij} represent the channel from transmit antenna j to receive antenna i. It has even been suggested by Andrews et al. [3] that, with three orthogonal components of the electric field and three of the magnetic field, it is possible to obtain six independent channels at a single point. While such statements in the far field are debatable, tripole antennas certainly offer advantages in the near field, if rich scattering is around the antenna sides as is typically the case for indoor environments and if orientation plays a role.

III. Measurement equipment and setup

A. Antenna design and structure

The antenna under test consists of three orthogonally aligned center-fed dipole radiators, each with a total length of $5.4\,\mathrm{cm}$ (see Fig. 2). Two printed circuit boards with a size of $10\,\mathrm{mm} \times 10\,\mathrm{mm}$, a thickness of $0.8\,\mathrm{mm}$ and a dielectric permittivity of $\epsilon_r = 4.7$ are used to carry the dipoles and ceramic SMD baluns (Johanson Technology 2450BL15B050). Parts of the two individual PCBs have been removed by cutting, to position the dipoles orthogonal to each other. A $50\,\mathrm{Ohm}$ Semi Rigid Cable is soldered to each of the unbalanced ports of the baluns.

978-1-4673-2220-1/12/$31.00

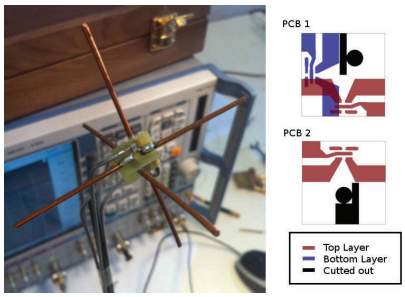

Fig. 2. Photograph of the antenna under test, with three orthogonal dipoles. On the right side the layouts of the two printed circuit boards are shown.

B. Measurement setup and scenarios

The measurement setup is depicted in Fig. 3. Channel frequency responses have been measured using a 4-port Rohde Schwarz Vector Network Analyzer (VNA). The three dipoles that make up Antenna Array 2 are directly connected to three of the VNA ports. Finally, Antenna Array 1 dipoles are connected to a RF switch, so that the signal can be transmitted sequentially to each element of this array. The measurement process is controlled by a Matlab script executed from a laptop, which is connected to the VNA by means of local area network (LAN).

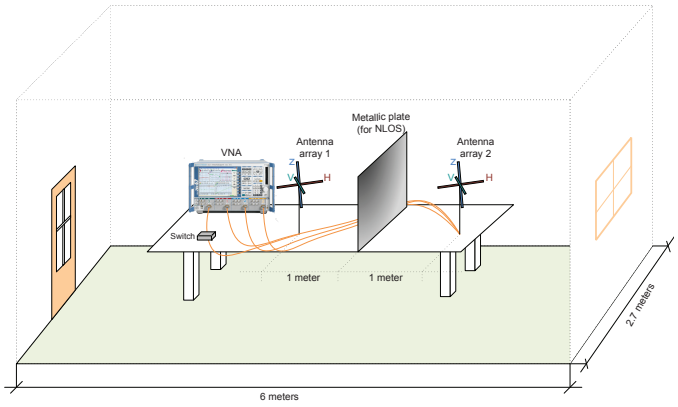

Fig. 3. Measurement setup for the transmissions over the air (Example: NLOS, 2 meters.

The measurements were performed in an office environment, which floor size is around $16\,\mathrm{m}^2$. We considered distances of 1 and 2 meters with line of sight (LOS) and non line of sight (NLOS) conditions (see Fig. 3). Antennas are $1.3\,\mathrm{m}$ above the floor; room height is $3.5\,\mathrm{m}$. The room was surrounded by brick walls and closed wooden/glass doors and filled with tables, chairs and so forth. The measurements were made at night to keep the environment as stable as possible, hence the frequency response did not vary in time. For NLOS measurements, the direct path was blocked with a large metallic plate situated between transmitter and receiver (see Fig. 3). The antenna arrays were arranged as shown in Fig. 3 prior to carrying out the measurement campaign. As can be seen, this orientation aligns H dipoles, so that the nulls in the radiation pattern of both antennas coincide.

IV. Channel Characterization and Measurements

The measurements were carried out by the VNA at a center frequency of $2.45\,\mathrm{GHz}$ and a bandwidth of $200\,\mathrm{MHz}$. Prior to carrying out the measurements, the VNA was thoroughly calibrated for each distance, including the effects of the coaxial cables and the switch. The Semi Rigid Cables could not be included in the calibration step since they were soldered to the balun (see Fig. 2). First, we obtain the S-parameters from the VNA. Since we have four ports, we receive three sets of 16 parameters, from each dipole connected to the switch. S_{11} and S_{21} parameters represent return losses and mutual couplings respectively. From the channel transfer functions, we can extract that the average powers of the orthogonal branches were $8\,\mathrm{dB}$ lower than the aligned ones. These results all confirm very well to the findings of Lee [6].

Fig. 4 presents the measured return losses (S_{11} parameter) and the worst-case isolation (S_{21} parameter). It can be observed that the worst-isolation is between port V and port H, which is $-10\,\mathrm{dB}$. The return losses are below $-3\,\mathrm{dB}$ in the frequency range 2.35 to $2.55\,\mathrm{GHz}$ in all cases and hence satisfactory for our purpose. From Fig. 4 we can observe the poor matching, possibly due to the unknown behavior of the Semi Rigid Cables.

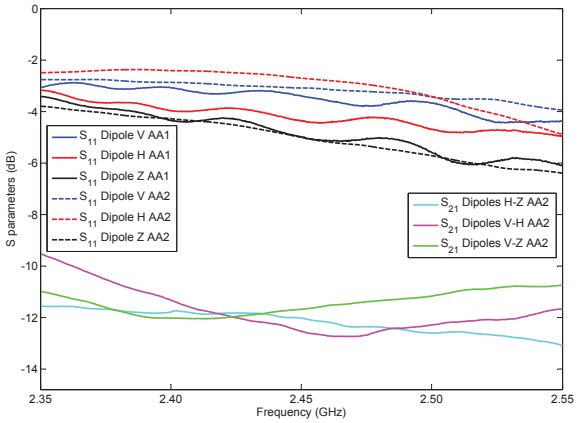

Fig. 4. Measured return losses and isolations. S_{11} represents return losses, S_{21} represents isolations. $AA1$ and $AA2$ refer to Antenna Array 1 and Antenna Array 2 respectively.

The output measured channel transfer functions were converted from the frequency domain to the time domain via inverse Fourier transform (IFFT). Note that a Hamming window is applied before IFFT in order to suppress sidelobes of the time-domain data [7]. In our case, the time resolution corresponds to the inverse of the measurement bandwidth, namely $1/(200\,\mathrm{MHz}) = 5\,\mathrm{ns}$. The number of points is 801 resulting in a frequency step size of $200\,10^6/801 \approx 250\,\mathrm{kHz}$. The resolution of the impulse response functions is reciprocal to the bandwidth multiplied by the additional width of the window, which results in an actual resolution of $10\,\mathrm{ns}$.

A. Cross Polarization Discrimination (XPD)

The XPD is defined as the ratio of the power received in desired polarization (transmitted) to the undesired (orthogonal) part. The propagation channel is characterized by a low

degree of cross-polarization coupling so that the three co-polarized communication branches (corresponding to the three polarization states) are virtually decoupled. Typically XPD values are high in channels with limited scattering such as LOS channels and much lower in NLOS channels. However high XPD values have been observed even in NLOS channels [8], in some measurement campaigns. For triple-polarized channels we have the following XPD definitions as

$$X_{ij} = \frac{E\left[|h_{ii}|^2\right]}{E\left[|h_{ji}|^2\right]} \quad i,j = v,h,z \quad i \neq j, \tag{1}$$

where $E[\cdot]$ denotes expectation. XPD ratios include the effect of both the antenna and the propagation link. Table I presents the XPD results extracted from the measurement campaign of the mean XPD for $2.45\,\mathrm{GHz}$ using (1).

	LOS		NLOS	
Tx/Rx Link	1 m.	2 m	1 m	2 m
H - V	9.27 dB	7.83 dB	1.91 dB	2.78 dB
V - H	4.78 dB	0.94 dB	7.12 dB	5.94 dB
V - Z	10.81 dB	7.22 dB	7.35 dB	8.34 dB
Z - V	10.67 dB	6.78 dB	4.16 dB	5.99 dB
Z - H	−0.86 dB	0.79 dB	9.48 dB	0.37 dB
H - Z	8.5 dB	9.39 dB	9.84 dB	3.21 dB

TABLE I
MEASURED MEAN XPDS.

In summary, results show that typical XPD values fall between 0 and $10\,\mathrm{dB}$ in most of the cases, and are surprisingly independent of other environment characteristics and of link distance, as happens in [9]. It is important to point out that the results are constrained to a particular orientation of the horizontal antennas at both ends. The difference between the XPDs of the vertically polarized and horizontally transmission highly depends on the specific propagation environment between the transmitter and the receiver.

B. Co-Polar-Ratio (CPR)

The CPR is the ratio of the signal levels of antennas with the same orientation compared to the ones with different orientations. The expressions of the CPR for a triple polarized MIMO configuration are

$$CPR_{ij} = \frac{E\left[|h_{ii}|^2\right]}{E\left[|h_{jj}|^2\right]} \quad i,j = v,h,z \quad i \neq j \tag{2}$$

The mean values obtained from the measurements, using (2) and taking logarithms, are presented in Table II. The rest of the combinations are the opposite of the ones in the table. We observe that the $H-V$ link remains negative (in LOS $1\,\mathrm{m}$ scenario) on average which means that the overall transmission of the V to V link is better than the H to H.

	LOS		NLOS	
Tx/Rx Link	1 m	2 m	1 m	2 m
H - V	8.56 dB	7.34 dB	−3.02 dB	2.22 dB
V - Z	3.48 dB	0.39 dB	6.79 dB	0.22 dB
H - Z	12.05 dB	7.73 dB	3.78 dB	2.41 dB

TABLE II
MEASURED MEAN CPRS.

C. Envelope Correlation

The performance of an antenna diversity system is also characterized by the envelope correlation. For a two-element antenna array it be simply calculated from the scattering parameters of the system [10], without knowing the radiation pattern.

$$\rho_e = \frac{|S_{XX}^* S_{XY} + S_{YX}^* S_{YY}|^2}{\left(1 - \left(|S_{XX}|^2 + |S_{YX}|^2\right)|\right)\left(1 - \left(|S_{YY}|^2 + |S_{XY}|^2\right)|\right)}$$

where S_{XX} and S_{YY} denote the input reflection coefficient for antenna X and antenna Y, respectively; S_{XY} and S_{XX} show the forward gain between two ports on different antennas, also reflect the mutual coupling between these two antennas. As can be seen from Table III, the antennas with the same orientation will be more correlated. We can state that the envelope correlation is not affected by distance or the LOS/NLOS conditions in the case that orientations differ. Regarding antennas with the same orientation, the $H-H$ combination presents a lower correlation than the $V-V$, and $Z-Z$ since the nulls of both dipoles almost match up. The existence of reflections matches up the results in NLOS.

	LOS		NLOS	
Tx/Rx Link	1 m.	2 m	1 m	2 m
V - V	−48 dB	−51 dB	−61 dB	−59 dB
H - H	−57 dB	−61 dB	−58 dB	−62 dB
Z - Z	−50 dB	−55 dB	−59 dB	−60 dB
V - H	−60 dB	−58 dB	−65 dB	−67 dB
V - Z	−59 dB	−59 dB	−62 dB	−69 dB
H - V	−57 dB	−61 dB	−60 dB	−63 dB
H - Z	−56 dB	−66 dB	−67 dB	−63 dB
Z - V	−59 dB	−61 dB	−65 dB	−69 dB
Z - H	−57 dB	−61 dB	−68 dB	−63 dB

TABLE III
MEASURED MEAN ENVELOPE CORRELATIONS.

1) Correlation coefficient measurements: We now study the complex correlation coefficient at both ends (i.e, we call them transmit and receive correlation coefficients). We calculate the transmit correlation among the transmit antennas for each receive antenna. Similarly, the receive correlation is calculated. This is carried out for all combinations of the Tx and Rx elements by computing the correlation coefficient between any two antennas X and Y according to (3)

$$\rho = \frac{E[XY^*] - E[X]E[Y^*]}{\sqrt{\left(E\left[|X|^2\right] - |E[X]|^2\right)\left(E\left[|Y|^2\right] - |E[Y]|^2\right)}} \tag{3}$$

As an example, Fig. 5 shows the cumulative distribution functions (CDFs) of the transmit correlation coefficients for

LOS, separation 1 meter. The curves are almost perfectly overlapping as for the other scenarios that have also been studied, resulting the same results in the mean. Receive correlation is found similarly.

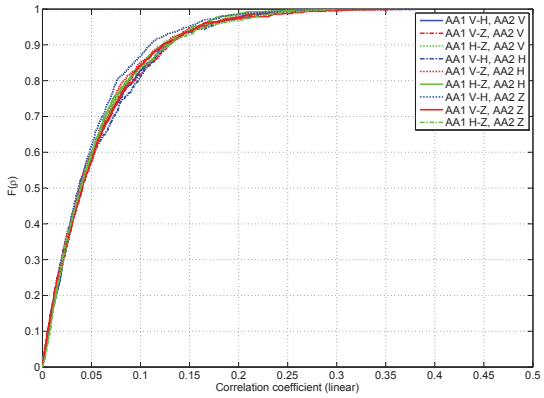

Fig. 5. Tx channel correlation coefficients CDF, LOS scenario, separation: 1 m.

It is found that $\rho < 0.3$ for the analyzed scenarios which demonstrates that the MIMO spatial subchannels are highly uncorrelated.

D. Ricean K-factor

The ratio of the coherent channel components, P_c, and the scattered channel components, P_s, is called Rician K-factor and is often represented in dB [11]: P_c has been extracted by considering the the complex baseband signal and P_s has been extracted by considering the variation of the baseband signal [12].

Tx/Rx Link	LOS		NLOS	
	1 m	2 m	1 m	2 m
V - V	12.21	8.73	4.63	6.40
V - H	3.69	10.77	7.18	6.44
V - Z	8.02	11.04	6.05	3.07
H - V	10.51	5.50	3.85	4.94
H - H	7.20	10.67	6.27	4.18
H - Z	12.60	3.09	3.46	3.09
Z - V	7.67	4.04	5.19	5.96
Z - H	11.44	4.44	6.59	6.75
Z - Z	13.48	4.57	3.48	4.98

TABLE IV
MEASURED K-FACTORS UNDER DIFFERENT CONDITIONS AND DISTANCES.

In general, the results show, as expected, that the K-factor decreases for NLOS scenarios.

E. Power delay profile (PDP)

The short time average PDP is obtained by averaging the magnitude squared of the channel, $\mathbf{h}$, over 801 frequencies, $L = 50$ snapshots and taking the sum over all $P = 16$ antenna to antenna channels, hence a static or wide sense stationary view of the channel conditions results. The RMS delay spread, τ_{rms}, can be extracted from the measured power PDP [13]. Table V shows the averaged values of the RMS delay spread. As expected, the delay spread increases in NLOS cases and, since the distances do not differ too much, it is in mean not affected by distance. In LOS and short distances, co-polar configurations have less RMS than cross-polar configurations.

Tx/Rx Link	LOS		NLOS	
	1 m	2 m	1 m	2 m
V - V	15.8 ns	19.5 ns	34.1 ns	25.1 ns
V - H	23.2 ns	20 ns	32.7 ns	38.1 ns
V - Z	18.8 ns	18.1 ns	21.6 ns	38.5 ns
H - V	14.6 ns	25.1 ns	20.5 ns	20 ns
H - H	20.4 ns	17.1 ns	16.5 ns	18 ns
H - Z	14.4 ns	24 ns	34.3 ns	28 ns
Z - V	24.3 ns	19 ns	25 ns	24 ns
Z - H	17.2 ns	22 ns	31 ns	19.3 ns
Z - Z	11 ns	17 ns	19 ns	22.2 ns

TABLE V
RMS DELAY SPREAD FOR THE DIFFERENT SCENARIOS.

V. CONCLUSIONS

The design and evaluation of two antenna arrays each consisting of three orthogonal co-located dipoles is presented. From the results, it can be concluded that the proposed antennas exhibit a good diversity performance due to low correlation values. Moreover, by exploiting polarization diversity, the proposed antennas can transmit information through three independent channels, being able to achieve higher capacities. The existence of nine possible choices among transmit and receive end suggest performing antenna selection to overcome deep fade situations. Apart from that, the presence of scattering objects around the receive array may cause components to leak from one polarization to another. This leads to a contribution of different polarizations into the same component at the receiver.

ACKNOWLEDGMENT

The authors would like to thank Philipp Gentner and Christoph F. Mecklenbräuker for his help and stimulating discussions. This work has been supported by MICINN (Spanish Ministry for Science and Innovation) under grants TEC2010-19545-C04-03 (COSIMA) and CONSOLIDER-INGENIO 2010 CSD2008-00010 (COMONSENS). It also has been supported by FPI grant BES-2008-002085. This work has also been funded by the Christian Doppler Laboratory for Wireless Technologies for Sustainable Mobility, KATHREIN-Werke KG, and A1 Telekom Austria AG. Also, it has been partially funded by the Higher Education Commission, Islamabad, Pakistan.

REFERENCES

[1] T. Svantesson and A. Ranheim, "Mutual Coupling Effects on the Capacity of Multi-Element Antenna Systems," in *Proceedings of the IEEE International Conference on Acoustics, Speech, and Signal Processing (ICASSP 01)*, April 2001, pp. 2485–2488.

[2] J. W. Wallace and M. A. Jensen, "The Capacity of MIMO Wireless Systems with Mutual Coupling," in *Proceedings of the IEEE Vehicular Technology Conference (VTC 02)*, 2002, pp. 696–700.

[3] M. R. Andrews, P. Mitra, and R. deCarvalho, "Tripling the capacity of wireless communications using electromagnetic polarization," *Nature*, vol. 409, no. 6818, pp. 316–318, 2001. [Online]. Available: http://www.ncbi.nlm.nih.gov/pubmed/11201734

[4] R. Tian and B. K. Lau, "Experimental verification of degrees of freedom for colocated antennas in wireless channels," *Antennas and Propagation, IEEE Transactions on*, vol. 60, no. 7, pp. 3416 –3423, july 2012.

[5] R. Vaughan, "Polarization diversity in mobile communications," *IEEE Trans. Veh. Technol.*, vol. 39, no. 3, pp. 177–186, August 1990.

[6] W. C. Y. Lee and Y. S. Yeh, "Polarization Diversity System for Mobile Radio," *IEEE Trans. Commun.*, vol. 20, no. 5, pp. 912–923, May 1972.
[7] P. F. M. Smulders and A. G. Wagemans, "Frequency-Domain Measurement of the Millimeter Wave Indoor Radio Channel," *IEEE Trans. Instrum. Meas.*, vol. 44, no. 6, pp. 1017–1022, Dec. 1995.
[8] X. Zhao, S. Geng, L. Vuokko, J. Kivinen, and P. Vainikainen, "Polarization Behaviours at 2.5 and 60 GHz for Indoor Mobile Communications," *Wireless Personal Communications*, vol. 27, pp. 99–115, 2003.
[9] V. Degli-Esposti, V.-M. Kolmonen, E. Vitucci, and P. Vainikainen, "Analysis and Modeling on Co- and Cross-Polarized Urban Radio Propagation for Dual-Polarized MIMO Wireless Systems," *IEEE Trans. Antennas and Propagation*, vol. 59, no. 11, pp. 4247 –4256, Nov. 2011.
[10] S. Blanch, J. Romeu, and I. Corbella, "Exact Representations of Antenna System Diversity Performance from Input Parameter Description," *Electronics Letters*, vol. 39, no. 9, May 2003.
[11] P. Soma, D. Baum, V. Erceg, R. Krishnamoorthy, and A. Paulraj, "Analysis and Modeling of Multiple-Input Multiple-Output (MIMO) Radio Channel Based on Outdoor Measurements Conducted at 2.5GHz for Fixed BWA Applications," in *Proc. ICC*, vol. 1, 2002, pp. 272 –276.
[12] F. Quintin, F. Bellens, A. Panahandeh, J.-M. Dricot, F. Dossin, F. Horlin, C. Oestges, and P. D. Donker, "A Time- Variant Statistical Channel Model for Tri-polarized Antenna Systems," *IEEE International Symposium on Personal Indoor and Mobile Radio Communications*, 2010.
[13] A. A. M. Saleh and R. A. Valenzuela, "A Statistical Model for Indoor Multipath Propagation," *J. Sel. Areas Commun.*, vol. 5, no. 2, pp. 128–137, Feb. 1987.